Demographic history of the Tibetan antelope *Pantholops hodgsoni* (chiru)

[1,2,3]Yu-Rong DU[§]   [1]Song-Chang GUO[§]   [4]Zhao-Feng WANG   [1]Hai-Xing CI   [1]Zhen-Yuan CAI
[4]Qian ZHANG   [1]Jian-Ping SU*   [4]Jian-Quan LIU*

[1](*Key Laboratory of Evolution and Adaptation of Plateau Biota, Northwest Institute of Plateau Biology, Chinese Academy of Sciences,* Xining 810001, China)
[2](*Graduate University of the Chinese Academy of Sciences,* Beijing 100049, China)
[3](*School of Life and Geography Science, Qinghai Normal University,* Xining 810008, China)
[4](*Key Laboratory of Arid and Grassland Ecology, School of Life Science, Lanzhou University,* Lanzhou 730000, China)

Abstract   The Tibetan antelope (chiru, *Pantholops hodgsoni*), a heavily poached species and symbol of the Qinghai-Tibetan Plateau (QTP), is noted worldwide for its special calving migration. This species originated in the early Quaternary and it is interesting to know how the following climatic oscillations affected its demographic dynamics in the climate-sensitive QTP. In this study, we analyzed the mitochondrial D-loop region from 312 individuals sampled in all of the six major populations. We found high rates of gene flow and little genetic differentiation between populations, suggesting that the calving migration may have homogenized the genetic pool of this species. Both mismatch distribution analyses and coalescent simulations suggested that this species experienced a demographic expansion approximately 600–200 Kyr following the retreat of the large glaciers developed in the QTP at 800–600 Kyr, rather than at the end of the last glacial age, as previously suggested, based on a limited sample size. In addition, we found evidence of a chiru population decrease probably related to the human settings at the QTP during the middle Holocene.
Key words   chiru, calving migration, demographic expansion, mitochondrial D-loop, Quaternary.

The Tibetan antelope (chiru, *Pantholops hodgsoni*) is a symbol of the Qinghai-Tibetan Plateau (QTP) and was one of the mascots for the Beijing 2008 Olympic Games (Fig. 1: A). It is also a highly poached species for the illegal wool trade (Schaller, 1998). This animal looks like an antelope, but it occurs far away from the African antelope species. Its skull characters are more similar to saiga than other antelope species. Recent morphological and molecular studies indicated that chiru is sister to the Caprinae (Gatesy et al., 1997; Lalueza-Fox et al., 2005). Available fossil data indicated that chiru had originated in the QTP during the early Pleistocene (approximately 2 Myr) (Gentry, 1992). Because the QTP is more sensitive to climatic changes than other regions in the world (Zheng, 1996), it is interesting to investigate how this ungulate animal responded to the Quaternary climatic oscillations. A growing body of studies from other temperate regions suggested that animal populations shrank and expanded in response to such climatic changes (Hewitt, 2000). In recent years, coalescence-based techniques have been developed to statistically examine such demographic histories of animal species (e.g. Drummond & Rambaut, 2007).

The calving migration of chirus has also received worldwide attention because a newly constructed railway intersected the migration routes between populations (Yang & Lin, 2008). Such migrations may have benefited migrants by providing access to more nutritious forage (Fryxell, 1987; McNaughton, 1988), avoidance of starvation by deep snow (Fryxell et al., 1988), reduction of the predation risk (Heptner et al., 1966), and dispersal of individuals when population growth is too fast (Child & Riche, 1969). This calving migration might promote genetic exchanges between populations and maintain all populations as a metapopulation. Chiru is currently listed as an endangered species and its continued survival is highly dependent on effective conservation measures (IUCN, 1996). Diverse measures have been adopted to protect this animal, including the prohibition of killing and smuggling, and the construction of calving migration corridors during the construction of the railway (Mallon & Kingswood, 2001; Yang & Lin, 2008; Mallon, 2009). A good knowledge of the genetic variation within and between populations of this species is crucial for its effective management. Ruan et al. (2005) studied the genetic diversity of this species and found low between-population differentiation based on the mitochondrial D-loop sequences of 57 individuals sampled from three sites. They suggested that this species experienced a rapid demographic expansion at the end of the Last Glacial Maximum (LGM, between
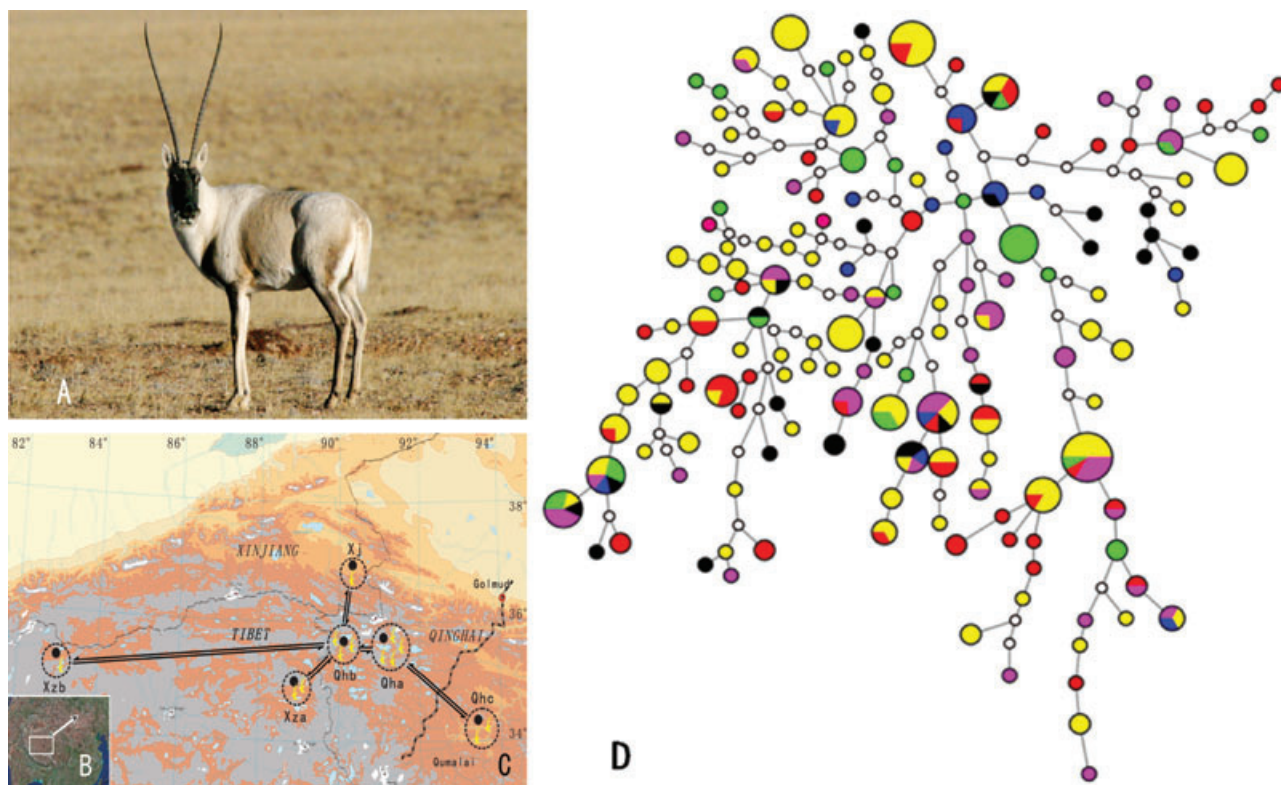
Fig. 1. Morphology and distribution of chirus and the mtDNA haplotype network. **A,** An adult male chiru. **B,** Distribution of chirus. **C,** Major distributions of chirus in winter, showing the five sampling sites (solid circles) and the calving migration routes (double lines with arrows) in summer according to our field observations and previous records. **D,** A median-joining network depicting the genetic relationship among haplotypes of the chiru. The sizes of the circles and colored segments are proportional to the haplotype frequencies in the datasets. Black, population Xj; blue, population Xzb; green, population Qhc; purple, population Xza; red, population Qhb; white, undetected intermediate haplotype states separated by one mutation step; yellow, population Qha.

20 and 10 Kyr), as did many other animal species in Europe and North America (Hewitt, 2000). However, recent studies suggested that the LGM had no effect on population dynamics of the QTP animals and population expansions of these alpine species started earlier (e.g. Qu et al., 2010; Tang et al., 2010). In this study, we analyzed the highly variable D-loop region of 312 individuals collected from the six main distribution regions of chiru (Qha, Qhb, Qhc, Xza, Xzb, and Xj) (Fig. 1: B, C). The main aims of the study were to: (i) examine in more detail the genetic variations within and between populations; and (ii) apply coalescent methods to simulate and reappraise the demographic history of this species.

1 Material and methods

1.1 Sample collection

Chirus reproduce from late June to early July. We followed the calving migrations of chiru during this period in 2003 and 2005. In general, most calving chirus migrate to two lakes in northwest QTP in summer (Fig. 1: C, Qha and Qhb) and some then return to their respective winter regions. The remaining chirus always stay in these two sites in winter. A total of 277 individuals were collected from six regions where chirus were killed by poachers in winter (Table 1, Fig. 1: B, C). The skins of these chirus were obtained through the local park guards. In addition, 35 sequences (GenBank accession numbers AY744081–AY744115) reported for Xzb and Xj (see Ruan et al., 2005) were added for the final analyses.

1.2 DNA extraction, amplification, and sequencing

Because most skins were not well preserved after being confiscated by park guards, we used two different methods to extract total genomic DNA: SDS–phenol/chloroform (Sambrook et al., 1989), and the QIAamp DNA Stool Mini Kit (Qiagen, Hilden, Germany). The decomposed DNA is unsuitable for amplifying long sequences by PCR. We synthesized two primers to amplify the highly variable region of the

Table 1   Details of populations, sampled numbers (*N*), haplotype numbers (*Nh*), and values of nucleotide divergence (*d*), nucleotide diversity (π), and haplotype diversity (*h*) in regional populations of chirus

Population	N (downloaded sequences from GenBank)	Nh	Pairwise differences (d)	Nucleotide diversity (π)	Haplotype diversity (h)
Qha	134	102	10.363 ± 4.757	0.0270 ± 0.0137	0.995 ± 0.002
Qhb	54	48	10.078 ± 4.678	0.0262 ± 0.0135	0.994 ± 0.006
Qhc	39	28	8.232 ± 3.900	0.0215 ± 0.0113	0.969 ± 0.017
Xza	31	24	8.727 ± 4.140	0.0228 ± 0.0120	0.983 ± 0.013
Xzb	28 (18)	26	11.025 ± 5.165	0.0288 ± 0.0151	0.995 ± 0.011
Xj	26 (17)	26	11.225 ± 5.266	0.0293 ± 0.0153	1.000 ± 0.011
Total	312 (35)	232	10.214 ± 4.676	0.0265 ± 0.0134	0.997 ± 0.001

D-loop for chirus: L-15960 5′-GGT AAT GTA CAT AAC ATT AAT G-3′ and H-16334 5′-CGA GAT GTC TTA TTT AAG AGG-3′. Amplifying and sequencing protocols followed Guo et al. (2006). No nuclear mitochondrial DNA was involved. The aligned sequences of 383–385 bp were used in the analyses, and all newly obtained sequences were submitted to GenBank (accession numbers DQ151533–DQ151799).

1.3   Data analysis

Haplotype relationships were obtained using median networks (Bandelt et al., 1995, 1999). Geographical association of haplotypes was tested by treating each population sample as a categorical variable (Hudson et al., 1992). The program MIGRATE v.2.1.3 (Beerli & Felsenstein, 2001; Beerli, 2004) was used to infer maximum likelihood migration rates among the six populations studied. Effective population sizes and gene flow estimates were obtained from F_{ST} values and were set as initial values. Arlequin v.3.0 (Excoffier et al., 2005) was used to estimate nucleotide diversity (π), haplotype diversity (*h*), hierarchical analysis of molecular variance, to calculate parameters, mismatch distributions, and to compute Fu's *Fs* test of selective neutrality (Fu, 1997). Values of Tajima's D (Tajima, 1989) were calculated from the total number of segregating sites and used to assess evidence for population expansion, under which negative values are expected (Aris-Brosou & Excoffier, 1996). We inferred the time to the most recent common ancestor (tMRCA) of all chirus by Bayesian coalescent analysis in BEAST v.1.5.2 (Drummond & Rambaut, 2007) under the relaxed uncorrelated clock model, calibrated using the time of divergence between sheep and goat of *ca* 5–7 Myr within the Caprinae (Savage & Russell, 1983; Carroll, 1988; Lalueza-Fox et al., 2005). The substitution model HKY+I+G was selected for Bayesian analyses by the ModelTest 3.7 (Posada & Crandall, 1998). Based on the estimated mutation rate and the observed generation time of 2 years, population expansions were further calculated on the basis of the equation $T = \tau/2u$ (Rogers & Harpending, 1992). Furthermore, we used the Bayesian Skyline Plot (BSP) approach to estimate the demographic history of chirus under tMRCA (Drummond & Rambaut, 2007). Piecewise-constant Skyline Model was selected. The number of groups (*m*) was set to 20. Bayesian MCMC was run for 300 million generations, and the initial 10% was discarded as "burn-in". The mutation rate in unit of substitution per site per year was coestimated along with the parameters of the BSP.

2   Results and discussion

Combining both our data and the published sequences, a total of 110 variable nucleotide sites and 232 haplotypes were identified in the samples investigated. Within each of the six populations, haplotype diversity values were nearly maximal (ranging from 0.9690 to 1.0000), whereas nucleotide diversity values were low (ranging from 0.02149 to 0.02931) (Table 1). No distinct haplotype group was identified by both network analyses and statistical parsimony techniques (Crandall & Templeton, 1996). A permutation categorical contingency analysis indicated no association with geographical location (population) ($P > 0.5$) of the identified haplotypes. Therefore, the identified haplotypes were randomly distributed within the sampled populations (Fig. 1).

Analysis of molecular variance analyses revealed that the total genetic variance was mainly located within populations (98.52% of the total variance) (Table 2),

Table 2   Hierarchical analysis of molecular variance in chirus

Source of variation	df	Sum of squares	Variance components	Percentage of variation	P
Among populations	5	32.453	0.075	1.48	0.003
Within populations	306	1528.905	4.996	98.52	0.000

Table 3 Estimates of gene flow (*Nem*) and theta among populations of chirus

Source population	Theta ($Ne\mu$)	Values of *Nem* for each recipient population					
		Qha	Qhb	Qhc	Xza	Xzb	Xj
Qha	1.74	—	25.75	7.53	34.77	15.50	13.05
Qhb	1.44	8.19	—	6.24	10.12	9.33	6.64
Qhc	0.93	2.14	1.80	—	4.47	2.01	4.02
Xza	0.59	4.31	2.43	2.94	—	1.91	1.36
Xzb	1.87	11.41	7.70	1.87	20.76	—	14.23
Xj	2.29	11.47	5.56	10.67	0.85	20.40	—

—, not applicable; μ, mutation rate; *m*, migration rate; *Ne*, effective population size of females.

suggesting high gene flow and little genetic differentiation between populations. Similarly, the maximum likelihood analyses indicated frequent exchanges of individuals per generation among 19 of 20 source-recipient comparisons (Table 3). At equilibrium, this gene flow through exchanging a few individuals per generation is sufficient to prevent genetic divergence between populations (Hartl & Clark, 1989) and must have repeatedly homogenized the genetic pool of this species. This genetic diversity pattern is totally different from the distinct phylogeographical structure revealed for other ungulate species (for example, roan antelope, Alpers et al., 2004).

Mismatch distribution analyses showed a unimodal frequency distribution of pair-wise differences in five of six populations and at the level of the whole metapopulation (Table 4, Fig. 2). Both Tajima's *D* and Fu's *Fs* values were negative and the tests for the latter values are highly significant (Table 4), suggesting demographic expansion (Fu, 1997). The tMRCA of all chirus was dated to 1.97 Myr before present (95% of the highest posterior density [HPD]: 3.41 to 0.83 Myr). This estimation is highly consistent with the early fossil record of chirus around 2 Myr in the early Quaternary (Gentry, 1992). The estimated mutation rate (6.88×10^{-8} substitutions per site per year (95% HPD: 3.44×10^{-8}–11.08×10^{-8} substitutions per site per year) is similar to that estimated for the roan antelope (Alpers et al., 2004). The estimated expansion dates of individual populations and the whole metapopulation were concordant, between 175 and 447 Kyr (Table 4). Even using the fastest mutation rate (32% per site per Myr) reported for steppe bison (Shapiro et al., 2004), all estimated expansions occurred before 50 Kyr, far earlier than the end of the LGM. This thus rejects the postglacial expansion hypothesis suggested elsewhere based on a limited sample size (Ruan et al., 2005). We further used BSP to simulate the demographic dynamics of chirus as their origin is estimated or recorded by fossil at 2 Myr before present. We found evidence of constant population size during the early-mid Quaternary, but after the end

Table 4 Mismatch distribution analyses, population expansion tests, and expansion dating in regional populations of chirus

Parameters	Qha	Qhb	Qhc	Xza	Xzb	Xj	Pooled
S	64	57	40	36	56	61	110
θ_0	5.00	3.10	0.90	5.36	5.37	5.31	4.91
θ_1	285.31	105.29	13.38	92.34	99999	148.28	205.94
τ (CI = 95%)	6.51 (3.87–15.80)	7.71 (4.73–15.09)	11.83 (2.74–23.73)	4.64 (2.82–16.51)	5.94 (3.36–16.26)	7.67 (4.10–18.09)	6.34 (3.73–15.90)
T (Kyr)	246 (146–596)	291 (178–570)	447 (103–896)	175 106–623	224 127–614	290 (155–683)	239 (141–600)
Goodness-of-fit test							
SSD	0.0036	0.0022	0.0043	0.0086	0.0040	0.0031	0.0016
P	0.3228	0.4867	0.9561	0.3153	0.6298	0.7421	0.4886
R	0.0039	0.0051	0.063	0.021	0.010	0.0056	0.0022
P	0.4831	0.6384	0.9858	0.1307	0.7230	0.9063	0.7913
Tajima's *D*	−0.4094	−0.7190	−0.3790	−0.2138	−0.9335	−1.0547	−1.2733
P	0.4034	0.2590	0.4117	0.4716	0.1802	0.1342	0.0714
Fu's *Fs*	−24.32	−24.61	−12.56	−10.26	−14.71	−18.02	−23.99
P	0.0000	0.0000	0.0005	0.0010	0.0000	0.0000	0.0018

The parameters of the model of sudden expansion (Rogers & Harpending, 1992) are presented as well as goodness-of-fit test to the model. *R*, raggedness indexes; SSD, sum of squared deviations. Tajima's (1989) *D* test values and their statistical significance are also given. *S*, number of polymorphic sites; θ_0, pre-expansion and θ_1, post-expansion population size; τ, time in number of generations, elapsed since the sudden expansion episode; *T*, the estimated expansion time, estimated according to mutation rate derived from this dataset: 6.88% substitutions per site per Myr.
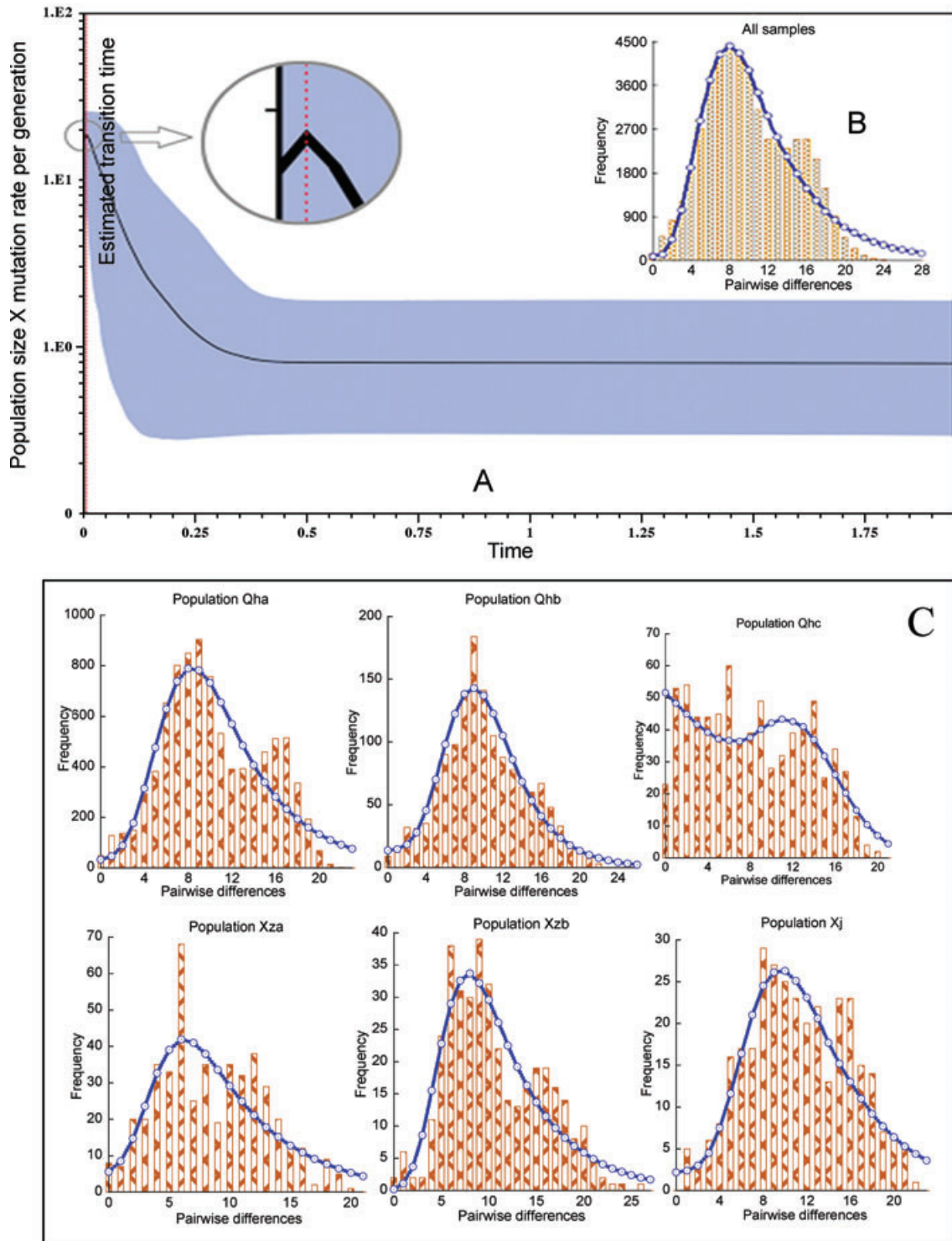
Fig. 2. Results of coalescent analysis using BEAST and mismatch distribution analysis. **A,** Bayesian skyline plot (m = 20) derived from all sequences of the chirus. The X-axis is in units of million years in the past and the Y axis is Ne × μ (effective population size × mutation rate per generation). Smoothed curves show mean and 95% of the highest posterior density (blue-shaded region) values for effective population size over time. Dashed vertical line represents the transition time, which is estimated at approximately 5 Kyr (4–6 Kyr). **B,** Mismatch distribution analyses of all samples. The histograms represent the observed frequencies of pairwise differences among haplotypes and the line shows the curve expected for a population that has expanded. **C,** Mismatch distribution analyses of six populations. The histograms represent the observed frequencies of pairwise differences among haplotypes and the line shows the curve expected for a population that has expanded.

of the largest glaciers (800–600 Kyr) developed in the QTP (Shi, 1998), a demographic expansion occurred until the mid Holocene. However, the population size began to decrease rapidly (negative growth) (Fig. 2), with a transition around 5 Kyr. These estimates and simulations together suggest that LGM had little effect on the demographic dynamics of chirus, as found for other QTP animals (e.g. Qu et al., 2010; Tang et al., 2010). It seems clear that the chiru populations began to expand earlier, probably when the largest glaciers in the QTP ended (Shi, 1998), then maintained in size until the early Holocene (Fig. 2). However, humans began to settle on the QTP at approximately 20 Kyr, and the number of immigrants from Northeast Asia increased rapidly at the end of the LGM (Zhao et al., 2009). The estimated Holocene transition time confirms that these human activities might have accounted for the decline of the chiru population size probably due to the following two facts. Chirus might have been killed for foods after the large-scale human colonization on the QTP. Increasing livestock grazing activities on the QTP (e.g. yak domestication during the early Holocene, Guo et al., 2006) should have intensified the resource competition between livestock animals and chirus (Cao et al., 2008, 2009).

References

Alpers DL, Jansen van Vuuren B, Arctander P, Robinson TJ. 2004. Population genetics of the roan antelope (*Hippotragus equinus*) with suggestions for conservation. Molecular Ecology 13: 1771–1784.

Aris-Brosou S, Excoffier L. 1996. The impact of population expansion and mutation rate heterogeneity on DNA sequence polymorphism. Molecular Biology and Evolution 13: 494–504.

Bandelt HJ, Forster P, Rohl A. 1999. Median-joining networks for inferring intraspecific phylogenies. Molecular Biology and Evolution 16: 37–48.

Bandelt HJ, Forster P, Sykes BC, Richards MB. 1995. Mitochondrial portraits of human populations using median networks. Genetics 141: 743–753.

Beerli P. 2004. MIGRATE: Documentation and program, part of LAMARC, version 2.0 [online]. Revised December 23, 2004. Available from http://evolution.gs.washington.edu/lamarc.html [accessed 29 September 2010].

Beerli P, Felsenstein J. 2001. Maximum-likelihood estimation of a migration matrix and effective population sizes in n subpopulations by using a coalescent approach. Proceedings of the National Academy of Sciences USA 98: 4563–4568.

Cao YF, Su JP, Lian XM, Zhang TZ, Cui QH. 2008. Food habits of Tibetan antelope (*Pantholops hodgsoni*) in the Kekexili Nature Reserve. Acta Theriologica Sinica 28: 14–19.

Cao YF, Zhang TZ, Lian XM, Cui QH, Deng DD, Su JP. 2009. Diet overlap among selected ungulates in Kekexili Region, Qinghai Province. Sichuan Journal of Zoology 28: 49–54.

Carroll RL. 1988. Vertebrate paleontology and evolution. New York: W.H. Freeman and Company.

Child G, Riche JL. 1969. Recent springbok treks (mass movements) in south-western Botswana. Mammalia 33: 499–504.

Crandall KA, Templeton AR. 1996. Applications of intraspecific phylogenetics. In: Harvey PH, Brown AJL, Smith JM, Nee S eds. New uses for new phylogenies. New York: Oxford University Press. 81–99.

Drummond AJ, Rambaut A. 2007. BEAST: Bayesian evolutionary analysis by sampling trees. BMC Evolutionary Biology 7: 214.

Excoffier L, Laval G, Schneider S. 2005. ARLEQUIN v.3.0: an integrated software package for population genetics data analysis. Evolutionary Bioinformatics 1: 47–50.

Fryxell J. 1987. Food limitation and demography of a migratory antelope, the white-eared kob. Oecologia 72: 83–91.

Fryxell JM, Greever J, Sinclair ARE. 1988. Why are migratory ungulates so abundant? American Naturalist 131: 781–798.

Fu YX. 1997. Statistical tests of neutrality of mutations against population growth, hitchhiking and background selection. Genetics 147: 915–925.

Gatesy J, Amato G, Vrba E, Schaller G, DeSalle R. 1997. A cladistic analysis of mitochondrial ribosomal DNA from the Bovidae. Molecular Phylogenetics and Evolution 7: 303–319.

Gentry A. 1992. The subfamilies and tribes of the family Bovidae. Mammal Review 22: 1–32.

Guo SC, Savolainen P, Su JP, Zhang Q, Qi DL, Zhou J, Zhong Y, Zhao XQ, Liu JQ. 2006. Origin of mitochondrial DNA diversity of domestic yaks. BMC Evolutionary Biology 6: 73.

Hartl DL, Clark AG. 1989. Principles of populations genetics. Sunderland: Sinauer Press.

Heptner V, Nasimovic A, Bannikov A. 1966. Die Saugetiere der Sowjetunion. 1. Paarhufer und Unpaarhufer. Jena: Gustav Fisher Verlag.

Hewitt GM. 2000. The genetic legacy of the Quaternary ice ages. Nature 405: 907–913.

Hudson RR, Boos DD, Kaplan NL. 1992. A statistical test for detecting geographic subdivision. Molecular Biology and Evolution 9: 138–151.

IUCN. 1996. Red list of threatened animals. Gland: IUCN.

Lalueza-Fox C, Castresana J, Sampietro L, Marques-Bonet T, Alcover JA, Bertranpetit J. 2005. Molecular dating of caprines using ancient DNA sequences of *Myotragus balearicus*, an extinct endemic Balearic mammal. BMC Evolutionary Biology 5: 70.

Mallon DP. 2009. *Pantholops hodgsonii*. In: The IUCN red list of threatened species. http://www.iucnredlist.org/apps/redlist/details/15967/0

Mallon DP, Kingswood SC. 2001. Global survey and regional action plans on antelope. Gland and Cambridge: IUCN.

McNaughton SJ. 1988. Mineral nutrition and spatial concentrations of African ungulates. Nature 334: 343–345.

Posada D, Crandall KA. 1998. MODELTEST: testing the model of DNA substitution. Bioinformatics 14: 817–818.

Qu Y, Lei F, Zhang R, Lu X. 2010. Comparative phylogeography of five avian species: implications for Pleistocene evolutionary history in the Qinghai-Tibetan plateau. Molecular Ecology 19: 338–351.

Rogers AR, Harpending H. 1992. Population growth makes waves in the distribution of pairwise genetic differences. Molecular Biology and Evolution 9: 552–569.

Ruan XD, He PJ, Zhang JL, Wan QH, Fang SG. 2005. Evolutionary history and current population relationships of the chiru (*Pantholops hodgsonii*) inferred from mtDNA variation. Journal of Mammalogy 86: 881–886.

Sambrook J, Fritsch EF, Maniatis T. 1989. Molecular cloning: A laboratory manual, 2nd edition. New York: Cold Spring Harbor Laboratory Press.

Savage DE, Russell DE. 1983. Mammalian paleofaunas of the world. London: Addison-Wesley Publishing Company.

Schaller GB. 1998. Wildlife of the Tibetan steppe. Chicago: University of Chicago Press.

Shapiro B, Drummond AJ, Rambaut A, Wilson MC, Matheus PE, Sher AV, Pybus OG, Gilbert MTP, Barnes I, Binladen J, Willerslev E, Hansen AJ, Baryshnikov GF, Burns JA, Davydov S, Driver JC, Froese DG, Harington CR, Keddie G, Kosintsev P, Kunz ML, Martin LD, Stephenson RO, Storer J, Tedford R, Zimov S, Cooper A. 2004. Rise and fall of Beringian steppe bison. Science 306: 1561–1565.

Shi YF. 1998. Evolution of the cryosphere in the Tibetan Plateau, China, and its relationship with the global change in the mid-Quaternary. Journal of Glaciology and Geocryology 20: 197–208.

Tajima F. 1989. Statistical methods to test for nucleotide mutation hypothesis by DNA polymorphism. Genetics 123: 585–595.

Tang LZ, Wang LY, Cai ZY, Zhang TZ, Ci HX, Lin GH, Su JP, Liu JQ. 2010. Allopatric divergence and phylogeographic structure of the plateau zokor (*Eospalax baileyi*), a fossorial rodent endemic to the Qinghai-Tibetan Plateau. Journal of Biogeography 37: 657–668.

Yang QS, Lin X. 2008. Tibetan wildlife is getting used to the railway. Nature 452: 810–811.

Zhao M, Kong QP, Wang HW, Peng MS, Xie XD, Wang WZ, Jiayang, Duan JG, Cai MC, Zhao SN, Cidanpingcuo, Tu YQ, Wu SF, Yao YG, Bandelt HJ, Zhang YP. 2009. Mitochondrial genome evidence reveals successful Late Paleolithic settlement on the Tibetan Plateau. Proceedings of the National Academy of Sciences USA 106: 21230–21235.

Zheng D. 1996. The system of physico-geographical regions of the Qinghai-Tibet (Xizang) Plateau. Science in China Series D: Earth Sciences 39: 410–417.